Tetrahedron 74 (2018) 407–417

Contents lists available at ScienceDirect

Tetrahedron

journal homepage: www.elsevier.com/locate/tet

Synthesis and properties of BF_2- & PO_2-complexes of mono *meso*-heterocycle substituted 25-oxasmaragdyrins and derivatives

Booruga Umasekhar, Mangalampalli Ravikanth*

Department of Chemistry, Indian Institute of Technology Bombay, Mumbai 400 076, India

ARTICLE INFO

Article history:
Received 20 October 2017
Received in revised form
21 November 2017
Accepted 4 December 2017
Available online 7 December 2017

Keywords:
Oxasmaragdyrin
PO_2- oxasmaragdyrin
Meso-heterocycle
Porphyrinoid macrocycles
Fluorescent compounds

ABSTRACT

BF_2- and PO_2-smaragdyrins containing one five membered heterocycle such as pyrrole, thiophene and furan at one of the *meso*-position of corresponding 25-oxasmaragdyrins were synthesized by treating the appropriate mono *meso*-heterocycle substituted 25-oxasmaragdyrin with $BF_3.OEt_2$ and $POCl_3$ respectively in CH_2Cl_2 under mild reaction conditions. All macrocycles were thoroughly characterized by HR-MS and 1D and 2D NMR spectroscopy. The presence of a five membered heterocycle in place of a six membered aryl group significantly alters the electronic properties of the smaragdyrin macrocycle as reflected in their spectral and electrochemical properties. The *meso*-pyrrole BF_2-smaragdyrin was subjected to a Vilsmeier-Haack reaction to prepare *meso*-(α-formyl pyrrolyl) BF_2-smaragdyrin which was subsequently used to prepare *meso*-(α-dipyrromethanyl pyrrolyl) BF_2-smaragdyrin. The further use of *meso*-heterocycle substituted BF_2- and PO_2-oxasmaragdyrins was demonstrated by treating *meso*-pyrrolyl BF_2-smaragdyrin with pentafluorobenzaldehyde in $CHCl_3$ under mild acid catalysed conditions to afford an unusual dipyrromethanyl bridged BF_2-smaragdyrin dyad which exhibits excellent photophysical properties.

1. Introduction

Porphyrins and related macrocycles containing one five membered *meso*-heterocycle such as pyrrole,[1–5] furan[6–11] and thiophene[12–20] are highly desirable building blocks to prepare several novel compounds. This is because the five membered *meso*-heterocycle can be easily functionalized and the functionalized *meso*-heterocycle substituted porphyrinoid macrocycles can be used to prepare variety of porphyrin based compounds with interesting physico-chemical properties.[12] Furthermore, the five membered heterocycle in place of six membered aryl groups at *meso*-position significantly alters the electronic properties of porphyrins and related macrocycles[9–12] Among the five membered heterocycle containing porphyrins, the *meso*-pyrrolyl porphyrins are more advantageous as pyrrole ring can be readily functionalized to extend the chemistry. A perusal of literature reveals that the reports on porphyrins and related macrocycles containing one and more pyrrole rings at *meso*-position(s) are very rare[1–5] whereas the reports on *meso*-thienyl[12–20] and *meso*-furyl[6–11] porphyrins are relatively common. Recently, we synthesized 22-oxacorrole **1** (Chart 1) containing one *meso*-pyrrolyl group[21] and was used to prepare unusual example of BODIPY (4,4-difluoro-4-bora-3a,4a-diaza-*s*-indacene) bridged 22-oxacorrole dyad.[22] This inspired us to design and prepare the porphyrin related macrocycles containing one or more five membered heterocycles at *meso*-positions and use these porphyrinoids as building blocks to synthesize a variety of interesting macrocycles with unusual properties.

Smaragdyrin(s) are 22-π aromatic pentapyrrolic macrocycles in which five pyrrole rings are connected via three *meso*-carbons and two direct pyrrole-pyrrole bonds.[23,24] However, the pentapyrrolic smaragdyrins[25,26] are not stable because of the presence of two direct pyrrole-pyrrole bonds which induces the strain in the macrocycle that lead to the decomposition. Interestingly, the *meso*-triaryl oxasmaragdyrins such as **2** which are resulted by substituting one of the pyrrole ring of the core with furan ring are noted to be quite stable and exhibit interesting physico-chemical properties.[27] The oxasmaragdyrins exhibit absorption and emission bands in 400–800 nm region with decent quantum yields and singlet state lifetimes and are stable under redox conditions. Few years back, we realized that the stability and properties of smaragdyrins can be enhanced further by complexation with BF_2- and PO_2 units to form BF_2-smaragdyrins[28] (**BF_2-2**) and PO_2-

* Corresponding author.
E-mail address: ravikanth@chem.iitb.ac.in (M. Ravikanth).

https://doi.org/10.1016/j.tet.2017.12.006
0040-4020/

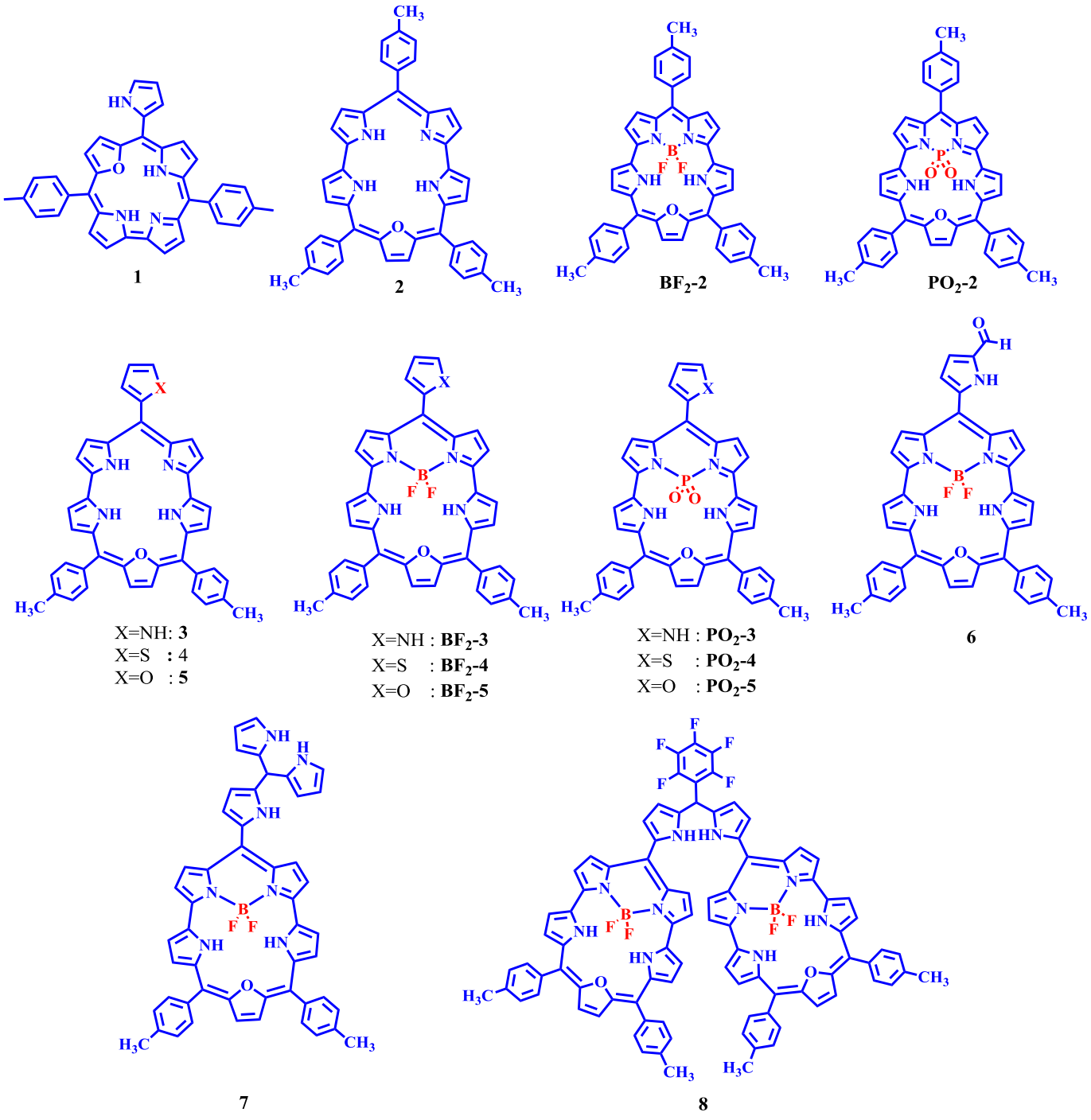

Chart 1. *Meso*-Heterocycle substituted free base, BF_2- and PO_2-smaragdyrins and their derivatives.

smaragdyrins[29] (**PO_2-2**) respectively (Chart 1). The BF_2- and PO_2-smaragdyrins possess the following novel features: (1) BF_2- and PO_2-smaragdyrins exhibit strong absorption band at ~720 nm with high extinction coefficient (e = ~50,000) in addition to other bands in Visible and Soret regions, (2) the complexes show one fluorescence band at ~730 nm with decent quantum yields and singlet state lifetimes and (3) they exhibit rich redox properties. Thus, BF_2- and PO_2 complexes of smaragdyrins are very stable under various conditions and possess very interesting photophysical and electrochemical properties. Recently, we prepared the *meso*-heterocycle substituted oxasmaragdyrins containing one five membered heterocyclic ring such as pyrrole **3**, thiophene **4** and furan **5** (Chart 1) at one of the *meso*-position and explored their spectral and electrochemical properties.[30] Our studies on mono *meso*-heterocycle substituted oxasmaragdyrins revealed that the electronic properties of smaragdyrins are greatly altered compared to *meso*-triaryl smaragdyrins **2**. However, these mono *meso*-heterocycle substituted oxasmaragdyrins **3**–**5** were found to be very unstable for functionalization of *meso*-heterocycle ring to extend the chemistry. Based on our previous studies, we know that the BF_2- and PO_2-smaragdyrins are quite stable for functionalization and these complexes also exhibit rich photophysical and redox

properties. With this idea in mind, in this paper, we synthesized BF_2- (**BF_2-3 - BF_2-5**) and PO_2- (**PO_2-3 - PO_2-5**) complexes of mono *meso*-heterocycle substituted oxasmaragdyrins and subjected the BF_2- complex of mono *meso*-pyrrolyl smaragdyrin **BF_2-3** for formylation reaction to afford *meso*-(α-formylpyrrolyl) BF_2-oxasmaragdyrin **6**.

The *meso*-(α-formylpyrrolyl) BF_2-oxasmaragdyrin **6** was further used to prepare *meso*-(α-dipyrromethanylpyrrolyl) BF_2-smaragdyrin **7**. The *meso*-(pyrrolyl) BF_2-smaragdyrin **BF_2-3** was also used directly as key synthon to prepare the rare example of dipyrromethanyl bridged smaragdyrin dyad **8**. The spectral and electrochemical properties of all BF_2- and PO_2- complexes of oxasmaragdyrins and derivatives were studied.

2. Results and discussion

The mono *meso*-heterocycle substituted oxasmaragdyrins **3**–**5** were prepared by 3 + 2 condensation of 16-oxatripyrrane[34] and appropriate *meso*-heterocycle substituted dipyrromethane[31–33] under mild acid catalysed conditions as reported by us. The BF_2 complexes **BF_2-3 - BF_2-5** were prepared by treating the appropriate *meso*-heterocycle substituted 25-oxasmaragdyrin **3**–**5** in CH_2Cl_2 with $BF_3.OEt_2$ in the presence of small amount of trimethylamine (Scheme 1).

The progress of the reaction was monitored by TLC which clearly showed the disappearance of spot corresponding to the starting material and appearance of more fluorescent spot of the required product. The crude compounds were purified by alumina column chromatography and afforded pure **BF_2-3** – **BF_2-5** in very high yields. Similarly, the PO_2 complexes **PO_2-3 - PO_2-5** were prepared by treating appropriate *meso*-heterocycle substituted smaragdyrins **3**–**5** in CH_2Cl_2 with $POCl_3$ in the presence of trimethylamine at 30 °C for 1 h. The formation of the desired PO_2 complexes **PO_2-3 - PO_2-5** was monitored by TLC and absorption spectroscopy (Scheme 1). The crude compounds were purified by silica gel column chromatography and afforded the PO_2 complexes **PO_2-3 - PO_2-5** as green solid in 80–85% yields. The BF_2 and PO_2 complexes of mono *meso*-heterocycle substituted smaragdyrins are freely soluble in common organic solvents and confirmed their identities by HR-MS. The complexes were characterized in detail by 1D and 2D NMR spectroscopy.

A representative ^{1}H NMR, ^{1}H-^{1}H COSY and ^{31}P NMR of **PO_2-5** is presented in Fig. 1 and comparison of ^{1}H NMR spectra of **3, BF_2-3** and **PO_2-3** in the selected region is presented in Fig. 2. In ^{1}H NMR spectrum of **PO_2-5**, the ten core protons, eight belongs to four pyrrole rings and two corresponds to furan protons appeared as five sets of resonances in 9.20–10.50 ppm region which were identified and assigned based on their location, integration, coupling constant and proton-proton cross-peak correlation in COSY NMR. The three *meso*-heterocycle protons were appeared as three separate resonances at 7.18, 8.13 and 8.35 ppm and the eight *meso*-aryl protons were appeared as two sets of multiplets at 7.60–8.50 ppm region. The ^{31}P NMR showed one strong singlet at −33.34 ppm supporting the formation of **PO_2-5**. The other PO_2 and BF_2 complexes were

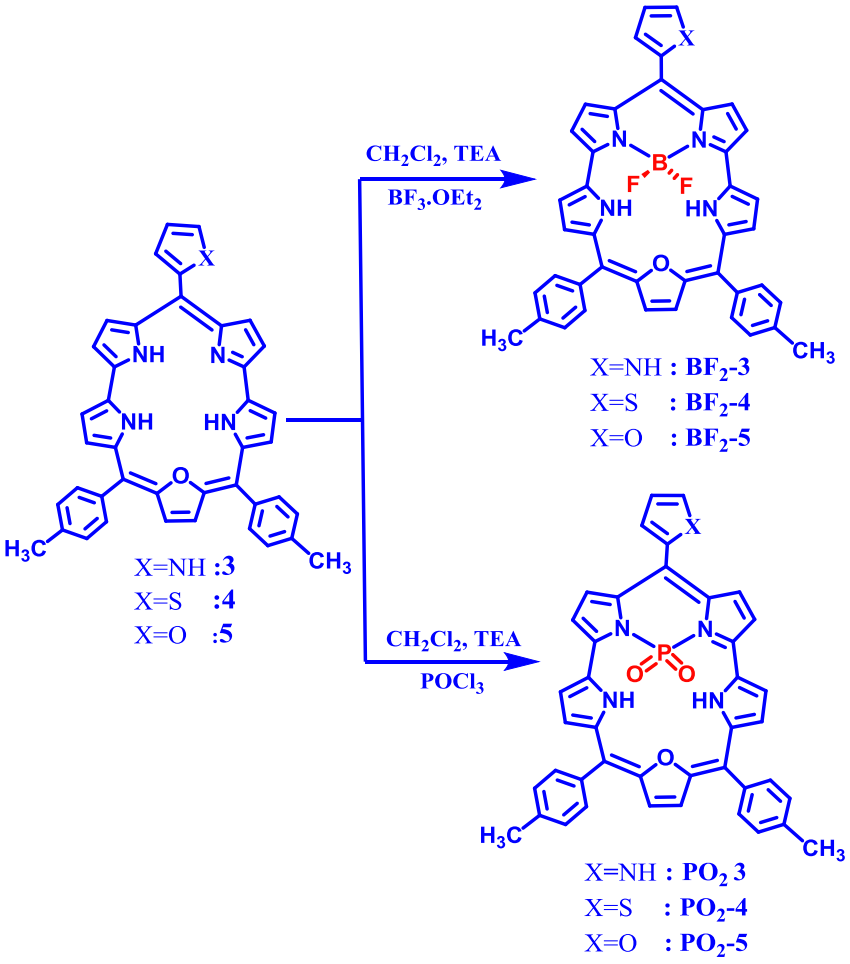

Scheme 1. Synthesis of various BF_2 & PO_2 complexes of mono *meso*-heterocycle substituted oxasmaragdyrins.

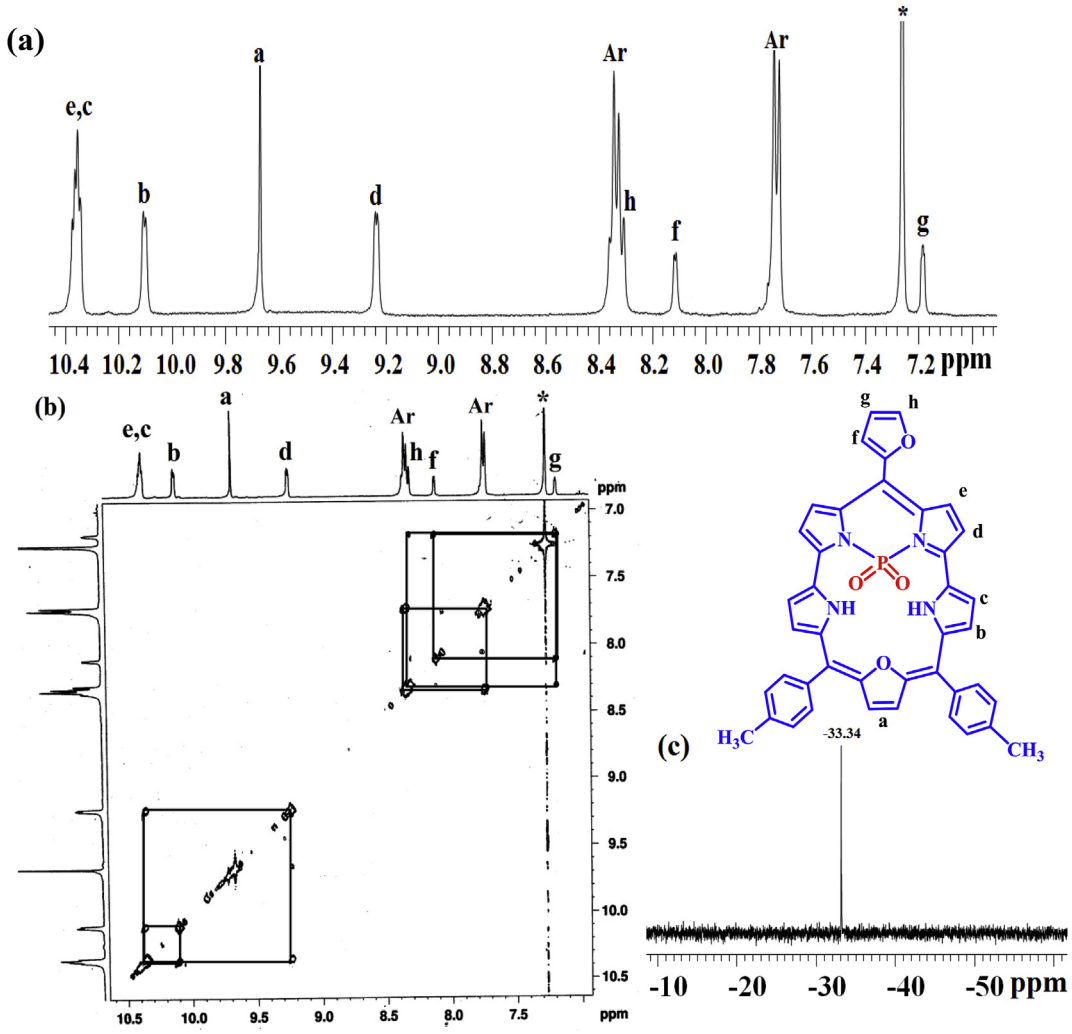

Fig. 1. (a) ^{1}H NMR, (b) ^{1}H-^{1}H COSY, (c) ^{31}P- NMR spectrum of compound **PO_2-5** recorded in $CDCl_3$ at room temperature.

similarly characterized by various multi-nuclear NMR techniques. The comparison of NMR of **3**, **BF_2-3** and **PO_2-3** clearly indicated that the ten core protons and other *meso*-aryl and *meso*-pyrrolyl protons of **BF_2-3** and **PO_2-3** experienced down-field shifts compared to **3** indicating that the insertion of BF_2- and PO_2 units into the smaragdyrin and the core alters the electronic properties significantly and maximum downfield shifts were observed for **PO_2-3**. For example, the NH proton of *meso*-pyrrolyl ring of compound **3** appeared at 9.50 ppm experienced downfield shift and appeared at 9.70 ppm in **BF_2-3** while it was further downfield shifted and appeared at 10.50 ppm in **PO_2-3**. Similarly, the two furan protons of smaragdyrin core which appeared as one singlet at 8.50 ppm in **3** experienced downfield shift and appeared at 9.40 ppm in **BF_2-3** and at 9.70 ppm in **PO_2-3**. Thus, BF_2- and PO_2-complexes of smaragdyrins exhibit altered electronic properties compared to free smaragdyrin.

The absorption, fluorescence and electrochemical properties of **BF_2-3** – **BF_2-5** and **PO_2-3 - PO_2-5** were studied and the relevant data are tabulated in Table 1. The comparison of normalized absorption spectra of **3**, **BF_2-3** and **PO_2-3** recorded in $CHCl_3$ is presented in (Fig. 3a). The **BF_2-3** and **PO_2-3** complexes showed similar absorption features like their corresponding free base smaragdyrins such as splitted Soret band in 440–500 nm region and three to four Q-type absorption bands in 590–750 nm region. However, the absorption bands of **BF_2-3** – **BF_2-5** and **PO_2-3 - PO_2-5** were bathochromically shifted with slight alterations in extinction coefficients compared to their corresponding free base smaragdyrins. Among BF_2 and PO_2-smaragdyrin complexes, the PO_2 complexes experienced more bathochromic shifts compared to BF_2-smaragdyrin complexes indicating that the electronic properties are more significantly altered in PO_2-smaragdyrins. Furthermore, the presence of furyl group at *meso*-position altered the electronic properties more significantly compared to thienyl and pyrrole groups in BF_2 and PO_2-smaragdyrin complexes as reflected in their absorption spectral properties. The steady state fluorescence properties of the **BF_2-3 - BF_2-5** and **PO_2-3 - PO_2-5** were studied in $CHCl_3$ (Table 1). The **BF_2-2** and **PO_2-2** complexes in general showed one strong fluorescent band at 703 and 714 nm respectively with decent quantum yields which are in the range of 0.15–0.18. The **BF_2-3 - BF_2-5** and **PO_2-3 - PO_2-5** complexes showed one strong fluorescence band in 730–750 nm region along with a shoulder band at 650–660 nm region. The fluorescence band of **BF_2-3 - BF_2-5** and **PO_2-3 - PO_2-5** complexes was red shifted compared to **BF_2-2** and **PO_2-2** complexes and maximum red shift in fluorescence band was observed for BF_2 and PO_2 complexes containing *meso*-furyl group.

All **BF_2-3 - BF_2-5** and **PO_2-3 - PO_2-5** complexes were decently fluorescent and quantum yield was dependent on the type of *meso*-

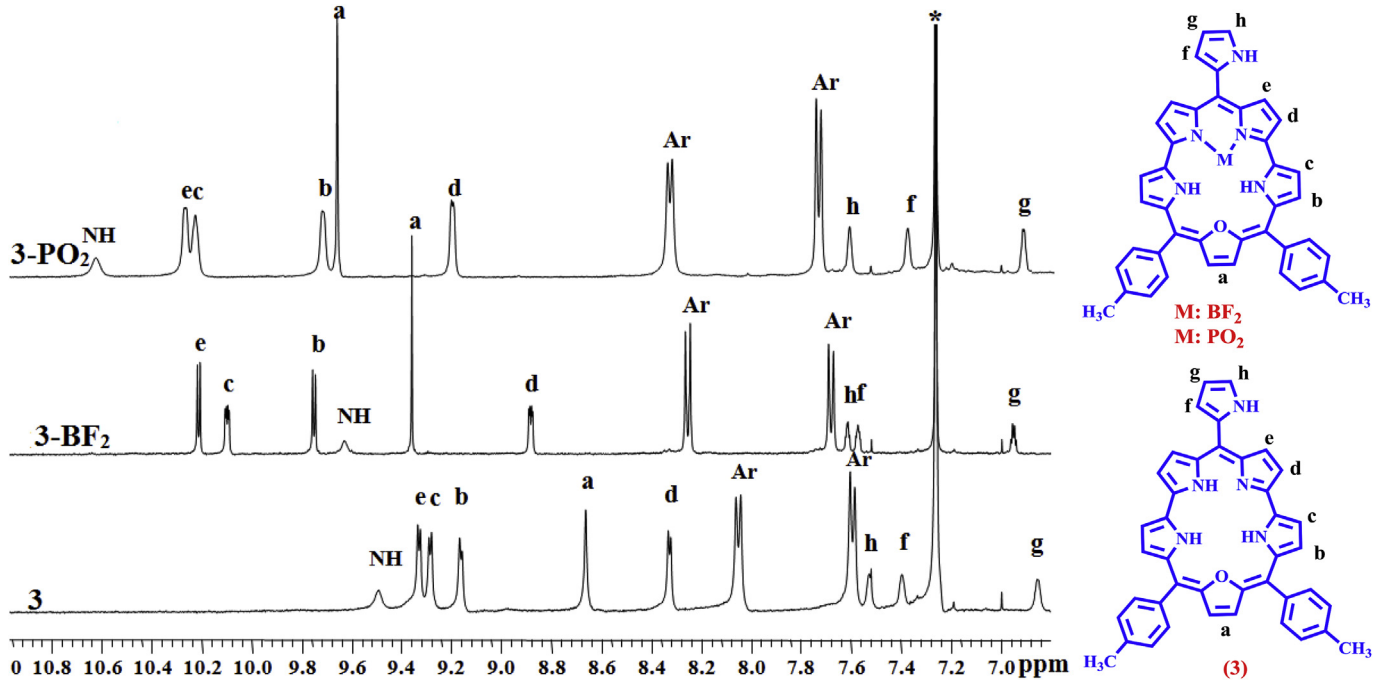

Fig. 2. Comparison of selected region of ^{1}H NMR spectra of compound **3**, **BF_2-3**, **PO_2-3** recorded in $CDCl_3$ recorded at room temperature.

Table 1
Photophysical data of **BF_2-2** – **BF_2-5** and **PO_2-2** – **PO_2-5** recorded in $CHCl_3$.

Compound	Soret bands, λ_{abs}/nm (log ε)	Q-bands, λ_{abs}/nm (log ε)	λ_{em}/nm	τ(ns)	Φ_f
BF_2-2	446(5.4), 475(5.1)	591(4.0), 629(sh), 647(4.2), 703(4.6)	703	4.7	0.15
BF_2-3	454(5.5), 482(5.1)	592(4.0), 631(sh), 655(4.2), 717(4.7)	729, 656	4.3	0.12
BF_2-4	446(5.3), 476(5.0)	590(3.9), 633(sh), 654(4.2), 709(4.4)	722, 650	4.0	0.09
BF_2-5	454(5.6),487(5.2)	593(4.2), 633(sh), 656(4.3), 722(4.7)	731, 656	4.1	0.08
PO_2-2	448(5.7), 486(5.3)	611(4.2), 642(4.1), 667(4.5),708(4.9)	714	4.3	0.18
PO_2-3	454(5.6), 490(5.3)	618(4.3), 643(4.2), 671(4.5),723(4.9)	740, 655	4.0	0.15
PO_2-4	456(5.7), 493(5.2)	611(4.2), 642(4.1), 665(4.4),739(4.8)	736, 649	4.3	0.12
PO_2-5	455(5.6), 494(5.4)	615(4.4), 644(4.2), 674(4.6),744(4.9)	743, 654	4.2	0.09

heterocycle group. The *meso*-thienyl and *meso*-furyl BF_2 and PO_2-smaragdyrin complexes were slightly less fluorescent than *meso*-pyrrolyl BF_2 and PO_2-smaragdyrin complexes. The singlet state lifetimes of BF_2 and PO_2-smaragdyrin complexes were measured using time-resolved single photon counting technique and a representative fluorescence decay profile is shown in (Fig. 3c). The fluorescence decays of BF_2 and PO_2-smaragdyrin complexes were fitted to single exponential with single state lifetime of ~4 ns. The singlet state lifetimes of BF_2 and PO_2-smaragdyrin complexes are almost in agreement with their quantum yield data.

The electrochemical properties of BF_2- and PO_2-smaragdyrin complexes were probed through cyclic voltammetry and differential pulse voltammetry by using 0.1 M tetrabutylammonium perchlorate (TBAP) as the supporting electrolyte with dichloromethane as solvent. The comparison of oxidation and reduction waves of **PO_2-5** and **BF_2-5** is shown in (Fig. 3d) and the relevant data of all compounds is presented in Table 2. The **BF_2-5** and **PO_2-5** showed two quasi-reversible oxidations and one irreversible reduction. In general, the *meso*-heterocycle substituted BF_2-smaragdyrins **BF_2-3-BF_2-5** and PO_2-smaragdyrins **PO_2-3-PO_2-5** showed macrocycle centered two quasi-reversible oxidations and one irreversible reduction like their *meso*-aryl counterparts such as **BF_2-2** and **PO_2-2** respectively.

The oxidation potentials of **BF_2-3 - BF_2-5** and **PO_2-3 - PO_2-5** were shifted towards less positive potential indicating that the *meso*-heterocycle substituted BF_2- and PO_2-smaragdyrins were easier to oxidize than *meso*-aryl BF_2-**(BF_2-2)** and PO_2-smargdyrins **(PO_2-2)**. Whereas the reduction potential of *meso*-heterocycle substituted BF_2- and PO_2-smaragdyrins were shifted towards more negative potential than *meso*-aryl BF_2- and PO_2-smaragdyrins indicating that the *meso*-heterocycle substituted BF_2- and PO_2-smaragdyrins are more electron rich than *meso*-aryl BF_2- and PO_2-smaragdyrins. Thus, the electrochemical properties indicated that the introduction of five membered heterocycle at *meso*-position makes these macrocycles more electron rich than their *meso*-aryl smaragdyrins.

2.1. Functionalization of meso-pyrrole substituted oxasmaragdyrins

The presence of five membered heterocycle at the *meso*-position of BF_2/PO_2-smaragdyrins is very useful to functionalize readily and the functionalized *meso*-heterocycle substituted BF_2/PO_2 smaragdyrins can be utilized to prepare a variety of fluorescent systems with potential applications in wide range of fields. We have taken *meso*-pyrrolyl substituted BF_2-smaragdyrin complex and subjected to Vilsmeier-Haack formylation reaction as shown in Scheme 2. Treatment of **BF_2-3** with Vilsmeier reagent in 1,2-dichloroethane at 65 °C for 30 min followed by column chromatographic purification

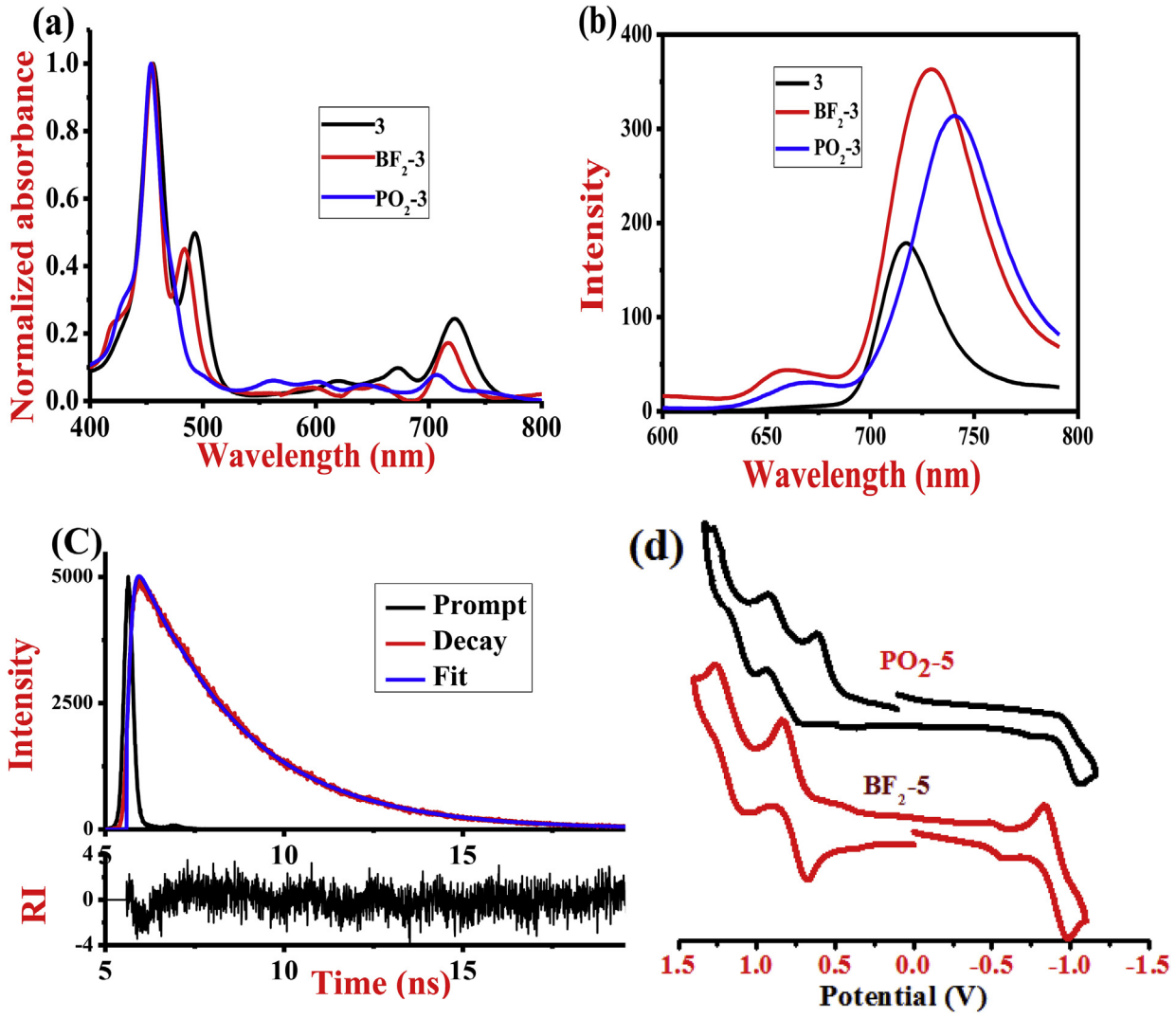

Fig. 3. (a) Comparison of normalized absorption spectra of **BF_2-3** and **PO_2-3** along with compound **3** recorded in $CHCl_3$. The concentrations used were 1×10^{-5} M; (b) Comparison of fluorescence spectra of **BF_2-3** and **PO_2-3** along with compound **3** recorded in $CHCl_3$. The concentrations used were 1×10^{-5} M. (c) Fluorescence-decay profile and the corresponding weighted residual distribution fit of compound **BF_2-5** in $CHCl_3$. (d) Comparison of cyclic voltammograms of **PO_2-5** and **BF_2-5** recorded in dichloromethane containing 0.1 M tetrabutylammonium perchlorate as the supporting electrolyte. The scan rate used was 50 mV s^{-1}.

Table 2
Electrochemical redox data (V) of compounds **BF_2-2 - BF_2-5** and **PO_2-2 - PO_2-5** recorded in dichloromethane containing 0.1 M TBAP as supporting electrolyte using scan rate of 50 mV/s. $E_{1/2}$ values reported are relative to SCE.

Compound	I	II	I
	E_{ox}(V)	E_{ox}(V)	E_{red}(V)
BF_2-2	0.80	1.22	−0.88
BF_2-3	0.75	1.17	−0.91
BF_2-4	0.76	1.18	−0.90
BF_2-5	0.78	1.20	−0.88
PO_2-2	0.74	1.12	−0.92
PO_2-3	0.50	0.80	−1.20
PO_2-4	0.49	0.81	−1.21
PO_2-5	0.52	0.83	−1.18

afforded *meso*-(α-formylpyrrolyl) BF_2-oxasmaragdyrin **6** in 85% yield. The formation of **6** was confirmed by resonance at 9.98 ppm corresponding to −CHO proton in ^{1}H NMR spectrum. Furthermore, the various protons of compound **6** were downfield shifted compared to **BF_2-3**. For example, the NH proton of *meso*-pyrrolyl group in compound **BF_2-3** appeared at 9.63 ppm experienced 0.90 ppm downfield shift in compound **6** and appeared at 10.53 ppm. To check the reactivity of formyl functional group at the α-position of *meso*-pyrrolyl group of **6**, we treated **6** with excess pyrrole under TFA catalysed conditions followed by column chromatographic purification affording *meso*-(α-dipyrromethanylpyrrolyl) BF_2-smaragdyrin **7** in 60% yield. The molecular ion peak at 801.32 in HR-MS confirmed the formation of compound **7**.

In ^{1}H NMR of **7**, the −CHO proton at 9.98 ppm was disappeared and new resonances corresponding to dipyrromethanyl moiety were appeared in 6–8 ppm region. In addition, all other protons including *meso*-pyrrolyl NH experienced slight upfield shifts in compound **7** compared to compound **6**. We also successfully synthesized an unusual dipyrromethanyl bridged BF_2 smaragdyrin dyad **8** using *meso*-pyrrolyl BF_2 smaragdyrin under simple acid catalysed conditions.

BF_2-3 with one equivalent of pentafluorobenzaldehyde in $CHCl_3$ in the presence of catalytic amount of TFA for 24 h at room temperature. The reaction progress was monitored by TLC analysis which showed the complete disappearance of spot corresponding to the starting precursor and appearance of new spot

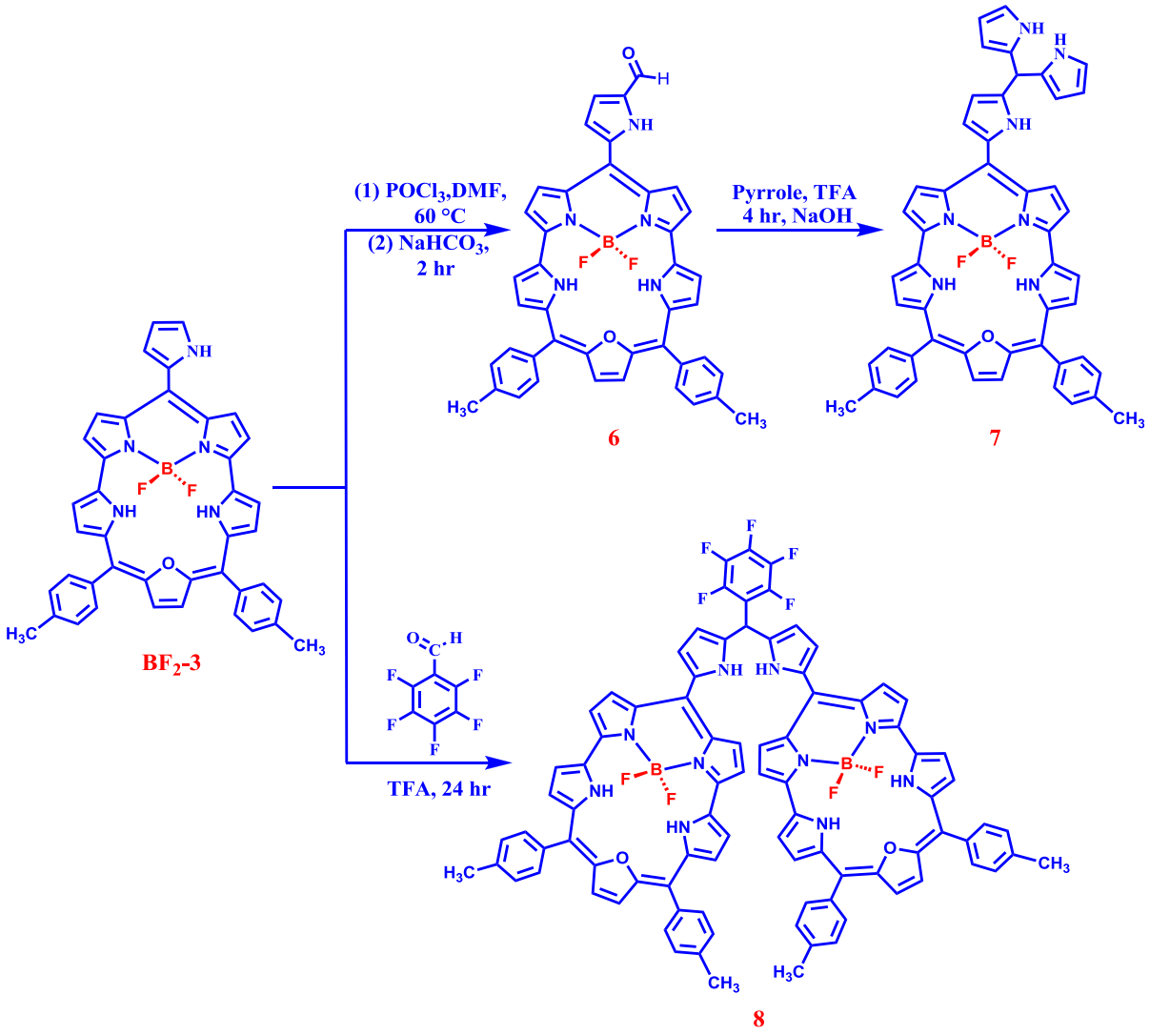

Scheme 2. Synthesis of *meso* (α-formylpyrrolyl) BF_2-smaragdyrin **6**, *meso*-(α-dipyrromethanyl pyrrolyl) BF_2-smaragdyrin **7** and dipyrromethanyl bridged BF_2-smaragdyrin dyad **8**.

corresponding to desired compound. Column chromatographic purification on alumina afforded the desired dipyrromethanyl bridged BF_2 smaragdyrin dyad **8** as green solid in 60% yield. The dyad **8** was characterized by 1D and 2D NMR spectroscopy and the comparison of ^{1}H NMR spectra of dyad **8** with its monomer, **BF_2-3** is shown in Fig. 4. In dyad **8**, the h-type pyrrole proton observed in monomer **BF_2-3** at 7.6 ppm was disappeared and an additional resonance corresponding to *meso*-dipyrrinyl CH proton appeared at 6.8 ppm confirming the formation of dyad **8**. Furthermore, the *meso*-pyrrolyl NH at 9.65 ppm in **BF_2-3** experienced downfield shift in dyad **8** and appeared at 10.1 ppm. All other protons also experienced slight shifts in dyad **8** compared to **BF_2-3**. The dyad **8** showed one single resonance at −1.0 ppm in ^{11}B NMR and four resonances at −141.40, −150.90, −155.85 and −161.28 ppm in ^{19}F NMR. In these, the resonance at −151 ppm was due to BF_2 unit whereas the other three resonances were due to *meso*-pentafluorophenyl group. The absorption spectrum of **8** showed almost same features like **BF_2-3** with slight alterations in extinction coefficients as shown in Fig. 4b. The fluorescence spectrum of dyad **8** was compared to its corresponding monomer **BF_2-3** in Fig. 4c. The **BF_2-3** showed two banded emission spectrum with peak maxima of 729 and 656 nm with a quantum yield of 0.12. However, the dyad **8** was weakly fluorescent and showed one broad fluorescence band at 713 nm with a quantum yield of 0.02. Furthermore, the dyad **8** showed featureless ill defined redox waves unlike its monomer **BF_2-3** indicating that the dyad **8** was not stable under redox conditions. Thus, the spectral and electrochemical studies indicated that there is a weak interaction between the two smaragdyrin units in dipyrromethanyl bridged smaragdyrin dyad **8**. Detailed studies are needed to understand the ground and excited state properties of dyad **8**.

3. Conclusions

In conclusion, we prepared mono *meso*-heterocycle substituted BF_2- and PO_2-oxasmaragdyrins by treating oxasmaragdyrins with $BF_3.OEt_2$ and $POCl_3$ respectively in CH_2Cl_2 under mild reaction conditions. The mono *meso*-heterocycle substituted 25-oxasmaragdyrins were prepared by [3 + 2] condensation of 16-oxatripyrrane with appropriate *meso*-heterocycle substituted dipyrromethane under mild acid catalysed conditions. The mono-*meso*-heterocycle substituted 25-oxasmaragdyrins absorbs and emits in near infra-red region with decent quantum yields and singlet state lifetimes. The presence of five membered heterocycle

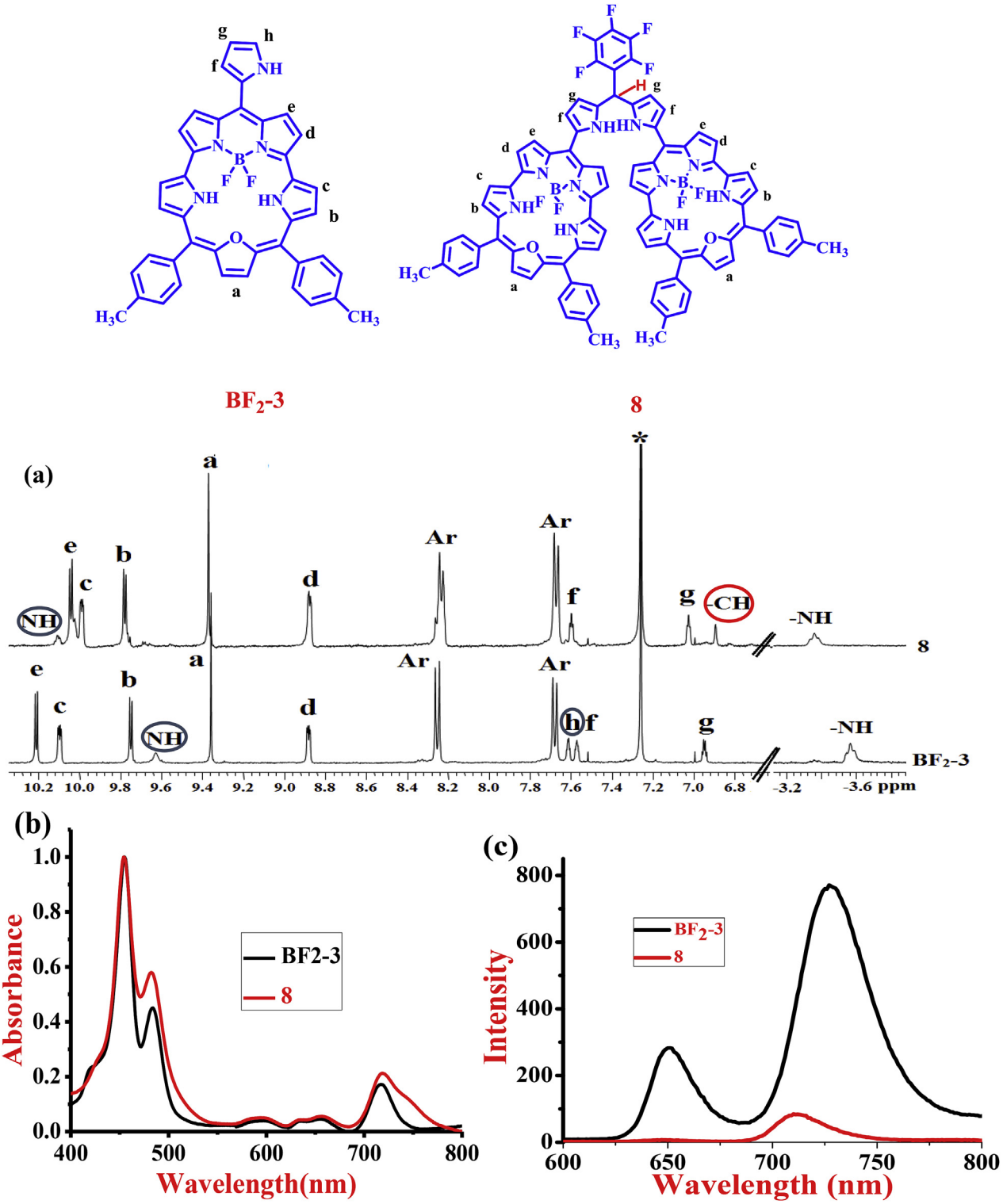

Fig. 4. Comparison of (a) selected region of ^{1}H NMR spectrum of compound **BF_2-3**, **8** recorded in $CDCl_3$ recorded at room temperature. (b) Absorption spectra of **BF_2-3** and **8** recorded in $CHCl_3$, the concentrations used were 1×10^{-5} M (c) Emission spectra of **BF_2-3** and **8** recorded in $CHCl_3$ the concentrations used were 1×10^{-5} M.

at *meso*-position of smaragdyrin alters the electronic properties of smaragdyrins significantly which was reflected in their spectral and electrochemical properties. To demonstrate the use of five membered heterocycle at *meso*-position of smaragdyrin, we carried out formylation reaction to prepare *meso*-(α-formyl pyrrolyl) BF_2-oxasmaragdyrin and the formyl group was subsequently used to prepare *meso*-(α-dipyrromethanyl pyrrolyl) BF_2-smaragdyrin. The *meso*-(α-dipyrromethanyl pyrrolyl) BF_2-smaragdyrin is a useful precursor to prepare several interesting BF_2-smaragdyrin based fluorescent compounds. Furthermore, we also prepared an unusual dipyrromethanyl bridged BF_2-smaragdyrin dyad by treating *meso*-pyrrolyl BF2-smaragdyrin with pentafluorobenzaldehyde under

mild acid catalysed conditions. Since BF_2- and PO_2-oxasmaragdyrins possess excellent photophysical properties, we hope that mono *meso*-heterocycle substituted BF_2- and PO_2-smaragdyrins will be used in design and synthesis of novel fluorescent compounds with wide range applications. Currently, we are exploring the potential use of mono *meso*-heterocycle substituted BF_2- and PO_2-oxasmaragdyrins to synthesize novel fluorescent compounds and study their properties and applications.

4. General experimental

4.1. Chemicals

THF and *n*-hexane was dried over sodium benzophenone ketyl, BF_3. Et_2O, 2,3-dichloro-5,6-dicyano-1,4-benzoquinone (DDQ) and TFA were used as obtained. All other chemicals used for the synthesis were reagent grade unless otherwise specified. Column chromatography was performed using silica gel and basic alumina obtained from Sisco Research Laboratories, India. All the solvents used were of analytical grade and were purified and dried by routine procedures immediately before use.

4.2. Instrumentation

The ^1H and ^1H-^1H COSY spectra were recorded on a Bruker 400 and 500 MHz NMR spectrometer. The ^{13}C NMR spectra were recorded on Bruker NMR spectrometer operating at 100.6 MHz. All of the NMR measurements were carried out at room temperature in deuterochloroform ($CDCl_3$) and TMS was used as an internal reference for the ^1H and ^{13}C chemical shifts in $CDCl_3$. The absorption and steady-state fluorescence spectra were obtained with Varian. The fluorescence spectra were recorded at 25 °C in a 1 cm quartz fluorescence cuvette. The fluorescence quantum yields (ϕ_f) were estimated from the emission and absorption spectra by comparative method at the excitation wavelength of 450 nm using H_2TPP ($\phi_f = 0.11$) as standard. The time-resolved fluorescence decay measurements were carried out at the magic angle using a picosecond-diode-laser-based, time-correlated single-photon-counting (TCSPC) fluorescence spectrometer (IBH, UK). All the decays were fit to a single exponential.

The Cyclic voltammetry (CV) studies were carried out with electrochemical system utilizing the three-electrode configuration consisting of a glassy carbon (working electrode), platinum wire (auxillary electrode) and saturated calomel (reference electrode) electrodes. The experiments were done in dry dichloromethane using 0.1 M tetrabutylammonium perchlorate as supporting electrolyte (TBAP). The half-wave potentials were measured using DPV and also calculated manually by taking the average of the cathodic and anodic peak potentials in the CV scans. All of the potentials were calibrated versus saturated calomel electrode by the addition of ferrocene as an internal standard, taking $E_{1/2}$ (Fc/Fc^+) = 0.51 V, vs SCE. The HR-MS spectra were recorded with a Bruker maxis impact 282001.00081 equipped with electrospray ionization and a TOF analyser.

4.3. General experimental for compounds **BF_2-3** to **BF_2-5**

A sample of appropriate *meso*-heterocycle substituted 25-oxasmaragdyrin **3**–**5** (0.157 mmol) was taken in CH_2Cl_2 (30 mL) and triethylamine (6.28 mmol) was added at room temperature. After 5 min, a catalytic amount of $BF_3.Et_2O$ (7.85 mmol) was added, and the stirring was continued at room temperature for 30 min. The reaction mixture was diluted with CH_2Cl_2 and washed thoroughly with 0.1 M NaOH aqueous solution. The organic layers were dried over Na_2SO_4, filtered, and the solvent was removed on a rotary evaporator under vacuum. The resulting crude product was purified by column chromatography on alumina, using petroleum ether/dichloromethane (70:30), and afforded pure compounds **BF_2-3 - BF_2-5** as a green solid.

4.3.1. Compound ***BF_2-3***

Yield 85%; ^1H NMR (400 MHz, $CDCl_3$, δ in ppm): 10.21 (d, 2H, $J = 4.30$ Hz, β-pyrrole H), 10.10 (d, 2H, $J = 3.92$ Hz, β-pyrrole H), 9.75 (d, 2H, $J = 4.50$ Hz, β-pyrrole H), 9.63 (brs, 1H, NH), 9.36 (s, 2H, β-furan H), 8.89 (d, 2H, $J = 4.00$ Hz, β-pyrrole H), 8.25 (d, 2H, $J = 7.8$ Hz, Ar), 7.70 (d, 2H, $J = 7.8$ Hz, Aromatic H), 7.61 (d, 1H, *meso*-pyrrole ring), 7.57 (d, 1H, $J = 2.92$ Hz, *meso*-pyrrole ring), 6.95 (d, 4H, $J = 7.60$ Hz, Ar), 2.80 (s, 6H, CH_3), −3.36 (m, −NH). ^{11}B NMR (128.37 MHz, $CDCl_3$, δ in ppm): −0.79. ^{19}F NMR (376.498 MHz, $CDCl_3$, δ in ppm 25 °C): −150.21. ^{13}C NMR (100 MHz, $CDCl_3$, δ in ppm): 150.1, 139.6, 138.0, 134.8, 131.2, 131.2, 130.8, 130.6, 128.4, 125.1, 123.9, 122.8, 120.7, 120.2, 107.2, 31.8. UV−vis (in $CHCl_3$, λ_{max}/nm, log ε) = 454(5.5), 482(5.1), 592(4.0), 631(sh), 655(4.2), 717(4.7), λ_{em} (nm) = 729, 656. HR-MS calcd for $C_{41}H_{30}BF_2N_5O$, *m/z* 657.2569, observed 657.2513.

4.3.2. Compound ***BF_2-4***

Yield 82%; ^1H NMR (400 MHz, $CDCl_3$, δ in ppm): 10.23 (d, 2H, $J = 4.30$ Hz, β-pyrrole H), 10.11 (d, 2H, $J = 4.25$ Hz, β-pyrrole H), 9.90 (d, 2H, $J = 4.50$ Hz, β-pyrrole H), 9.49 (s, 2H, β-furan H), 9.00 (d, 2H, $J = 4.25$ Hz, β-pyrrole H), 8.25 (d, 4H, $J = 7.80$ Hz, Ar), 7.70 (d, 4H, $J = 7.70$ Hz, Ar), 7.59 (d, 1H, $J = 3.24$ Hz, *meso*-thiophene ring), 7.49 (d, 1H, $J = 1.64$ Hz, *meso*-thiophene ring), 7.02 (dd, 1H, $J = 3.24$ Hz, *meso*-thiophene ring), 2.60 (s, 6H, CH_3), −3.85 (m, −NH). ^{11}B NMR (128.37 MHz, $CDCl_3$, δ in ppm): −0.96, ^{19}F NMR (376.498 MHz, $CDCl_3$, δ in ppm 25 °C): −151.9. ^{13}C NMR (100 MHz, $CDCl_3$, δ in ppm): 149.9, 137.9, 134.3, 132.3, 130.6, 128.3, 124.9, 124.8, 121.6, 120.3, 119.9, 106.8, 21.8. UV−vis (in $CHCl_3$, λ_{max}/nm, log ε) = 446(5.3), 476(5.0), 590(3.9), 633(sh), 654(4.2), 709(4.4). λ_{em} (nm) = 722, 650. HR-MS calcd for $C_{41}H_{29}BF_2N_4OS$ $(M+H)^+$ *m/z* 674.2123, observed 674.2125.

4.3.3. Compound ***BF_2-5***

Yield 80%; ^1H NMR (400 MHz, $CDCl_3$, δ in ppm): 10.35 (d, 2H, $J = 4.12$ Hz, β-pyrrole H), 10.25 (d, 2H, $J = 4.32$ Hz, β-pyrrole H), 10.05 (d, 2H, $J = 4.28$ Hz, β-pyrrole H), 9.49 (s, 2H, β-furan H), 9.00 (d, 2H, $J = 4.32$ Hz, β-pyrrole H), 8.35 (d, 1H, $J = 2.50$ Hz, *meso*-furan ring), 8.30 (d, 4H, $J = 7.75$ Hz, Ar), 7.80 (d, 1H, $J = 6.35$ Hz, *meso*-furan ring), 7.71 (d, 4H, $J = 7.76$ Hz, Ar), 7.25 (dd, 1H, $J = 5.85$ Hz, *meso*-furan ring), 2.80 (s, 6H, CH_3). ^{11}B NMR (128.37 MHz, $CDCl_3$, δ in ppm): −0.78, ^{19}F NMR (376.498 MHz, $CDCl_3$, δ in ppm 25 °C): −150.98. ^{13}C NMR (100 MHz, $CDCl_3$, δ in ppm): 150.0, 138.0, 134.4, 132.5, 132.0, 131.5, 131.1, 130.7, 128.4, 125.0, 124.7, 121.7, 120.4, 120.0, 106.9, 21.8. UV−vis (in $CHCl_3$, λ_{max}/nm, log ε) = 454(5.6), 487(5.2), 593(4.2), 633(sh), 656(4.3), 722(4.7), λ_{em} (nm) = 731, 656. HR-MS calcd for $C_{41}H_{29}BF_2N_4O_2$ *m/z* 658.2360, observed 658.2353.

4.4. General experimental for compounds **PO_2-3 - PO_2-5**

Sample of appropriate *meso*-heterocycle substituted 25-oxasmaragdyrin **3**–**5** (0.0946 mmol) was taken in a round-bottomed flask in CH_2Cl_2 and triethylamine (0.946 mmol) was added to it. $POCl_3$ (1.892 mmol) was added, and the reaction mixture was refluxed at 30 °C for 30 min. The reaction was quenched by adding ice water, and the compound was extracted with CH_2Cl_2. The combined organic layers were washed thoroughly with water and dried over Na_2SO_4. Silica gel column chromatographic purification of crude compound using petroleum ether/CH_2Cl_2 (1:1) as the eluent afforded compound **PO_2-3 - PO_2-5** as a green solid.

4.4.1. Compound ***PO$_2$-3***

Yield 85%; ^{1}H NMR (400 MHz, $CDCl_3$, δ in ppm): 10.63 (bs, 1H, NH), 10.27 (d, 2H, J = 2.2 Hz, β-pyrrole H), 10.23 (d, 2H, J = 3.92 Hz, β-pyrrole H), 9.72 (d, 2H, J = 3.92 Hz, β-pyrrole H), 9.66 (s, 2H, β-furan H), 9.20 (d, 2H, J = 2.60 Hz, β-pyrrole H), 8.33 (d, 4H, J = 7.30 Hz, Ar), δ 7.73 (d, 4H, J = 7.60 Hz, Ar), 7.61 (d, 1H, *meso*-pyrrole ring), 7.37 (d, 1H, J = 2.92 Hz, *meso*-pyrrole ring), 6.91 (dd, 1H, *meso*-pyrrole ring), 2.83 (s, 6H, CH_3), −3.85 (m −NH). ^{31}P{^{1}H} NMR (202.46 MHz, $CDCl_3$, δ in ppm): −32.69. ^{13}C NMR (100 MHz, $CDCl_3$, δ in ppm): 149.9, 138.0, 134.3, 132.8, 132.0, 131.5, 131.1, 130.7, 128.4, 125.0, 123.7, 121.6, 120.4, 120.0, 106.9, 21.8. UV−vis (in $CHCl_3$, λ_{max}/nm, log ε) = 454(5.6), 490(5.3), 618(4.3), 643(4.2), 671(4.5), 723(4.9), λ_{em} (nm) = 740, 655. HR-MS calcd for $C_{41}H_{31}N_5O_3P$, *m/z* 672.2154, observed 672.2159.

4.4.2. Compound ***PO$_2$-4***

Yield 82%; ^{1}H NMR (500 MHz, $CDCl_3$, δ in ppm): 10.29 (d, 2H, J = 4.25 Hz, β-pyrrole H), 10.15 (d, 2H, J = 4.25 Hz, β-pyrrole H), 9.80 (d, 2H, J = 4.20 Hz, β-pyrrole H), 9.35 (s, 2H, β-furan H), 8.88 (d, 2H, J = 4.25 Hz, β-pyrrole H), 8.25 (d, 4H, J = 7.68 Hz, Ar), 7.77 (d, 1H, J = 3.24 Hz, *meso*-thiophene ring), 7.61 (d, 4H, J = 7.70 Hz, Ar), 7.50 (dd, 1H, J = 3.24, 1.6 Hz, *meso*-thiophene ring), 7.00 (d, 1H, J = 1.64 Hz, *meso*-thiophene ring), 2.67 (s, 6H, CH_3), −1.85 (m, −NH), ^{31}P{^{1}H} NMR (202.46 MHz, $CDCl_3$, δ in ppm): −32.78. ^{13}C NMR (100 MHz, $CDCl_3$, δ in ppm): 149.9, 137.9, 134.32, 132.5, 132.0, 131.4, 131.0, 130.6, 128.4, 125.0, 123.6, 121.6, 120.3, 119.9, 106.9, 21.8. UV−vis (in $CHCl_3$, λ_{max}/nm, log ε) = 456(5.7), 493(5.2), 611(4.2), 642(4.1), 665(4.4), 739(4.8), λ_{em} (nm) = 736, 649. HR-MS calcd for $C_{41}H_{30}N_4O_3PS$ $(M+H)^+$ *m/z* 689.1777, observed 689.1771.

4.4.3. Compound ***-PO$_2$-5***

Yield 80%; ^{1}H NMR (400 MHz, $CDCl_3$, δ in ppm): 10.37 (d, 2H, J = 4.12 Hz, β-pyrrole H), 10.34 (d, 2H, J = 4.32 Hz, β-pyrrole H), 10.10 (d, 2H, J = 4.28 Hz, β-pyrrole H), 9.67 (s, 2H, β-furan H), 9.23 (d, 2H, J = 4.32 Hz, β-pyrrole H), 8.35 (d, 1H, J = 2.50 Hz, *meso*-furan ring), 8.35 (d, 1H, J = 2.50 Hz, *meso*-furan ring), 8.11 (d, 4H, J = 2 Hz, Ar), 7.73 (d, 4H, J = 7.76 Hz, Ar), 7.18 (d, 1H, J = 1.8 Hz, *meso*-furan ring), 2.82 (s, 6H, CH_3), −1.5 (m −NH). ^{31}P{^{1}H} NMR (202.46 MHz, $CDCl_3$, δ in ppm): −33.34. ^{13}C NMR (100 MHz, $CDCl_3$, δ in ppm): 150.8, 138.8, 135.2, 132.9, 132.3, 131.5, 129.2, 125.8, 121.5, 124.5, 122.5, 121.2, 120.8, 107.7, 21.8. UV−vis (in $CHCl_3$, λ_{max}/nm, log ε) = 455(5.6), 494(5.4), 615(4.4), 644(4.2), 674(4.6), 744(4.9), λ_{em} (nm) = 743, 654, HR-MS calcd for $C_{41}H_{30}N_4O_4P$, *m/z* 673.1995, observed 673.1999.

4.5. Compound ***6***

A mixture of DMF (41.8 mmol) and $POCl_3$ (38.0 mmol) was stirred at room temperature under nitrogen for 5 min. 1,2-Dichloroethane (8 mL) was added to it and the reaction mixture was stirred for 15 min at room temperature. Compound **BF$_2$-3** (1.9 mmol) in 1, 2-dichloroethane was added dropwise via a dropping funnel to the reaction mixture over a period of 30 min at room temperature. The reaction mixture was then warmed to 65 °C; stirred for 30 min and brought to room temperature. A saturated solution of $NaHCO_3$ was added and the reaction mixture was further stirred for 3 h at room temperature. The reaction mixture was extracted with CH_2Cl_2 and the collected organic layers were dried over Na_2SO_4. The solvent was removed on a rotary evaporator. The crude product was purified by alumina column chromatography using petroleum ether/dichloromethane (90/10) and the pure compound **6** was afforded as a light greenish solid in 85% yield. ^{1}H NMR (400 MHz, $CDCl_3$, δ in ppm): δ10.53 (bs, 1H, NH),10.46 (d, 2H, J = 4.12 Hz, β-pyrrole H), 10.32 (d, 2H, J = 4.32 Hz, β-pyrrole H), 9.98 ppm (bs, 1H, −CHO),9.87 (d, 2H, J = 4.28 Hz, β-pyrrole H), 9.57 (s, 2H, β-furan H), 9.11 (d, 2H, J = 4.32 Hz, β-pyrrole H), 8.32 (d, 1H, J = 2.50 Hz, *meso*-furan ring), 7.72 (d, 4H, J = 7.75 Hz, Ar), 7.67 (d, 4H, J = 7.76 Hz, Ar), 7.52 (d, 1H, J = 6.35 Hz, *meso*-furan ring), 7.00 (dd, 1H, J = 5.85 Hz, *meso*-furan ring), 1.41 (s, 6H, CH_3) −4.20 (m, −NH). ^{11}B NMR (160.46 MHz, $CDCl_3$, δ in ppm): −0.74, ^{19}F NMR (470 MHz, $CDCl_3$, δ in ppm 25 °C): −148.0.

4.6. Compound ***7***

Solution of an aldehyde **6** (1.7 mmol) and pyrrole (68.0 mmol), a catalytic amount of TFA (0.17 mmol) was added under a nitrogen atmosphere in CH_2Cl_2 and the reaction mixture was stirred at room temperature for 6 h. The progress of the reaction was monitored by TLC and absorption spectroscopy. A saturated solution of NaOH was added to quench the reaction. The reaction mixture was extracted with CH_2Cl_2 and the collected organic layers were dried over Na_2SO_4. The solvent was removed on a rotary evaporator. The crude product was purified by column chromatography using petroleum ether/dichloromethane (60/40) and the pure compound **7** was afforded as a greenish solid in 60% yield. ^{1}H NMR (500 MHz, $CDCl_3$, δ in ppm): 10.26 (d, 2H, J = 4.35 Hz, β-pyrrole H), 10.14 (d, 2H, J = 3.92 Hz, β-pyrrole H), 9.80 (d, 2H, J = 3.92 Hz, β-pyrrole H), δ 9.67 (bs, 1H, NH), 9.39 (s, 2H, β-furan H), 8.91 (d, 2H, J = 4.00 Hz, β-pyrrole H), 8.26 (d, 4H, J = 7.45 Hz, Ar), 7.71 (d, 4H, J = 7.45 Hz, Ar), 7.67 (d, 1H, *meso*-pyrrole ring), 7.61 (d, 1H, J = 2.92 Hz, *meso*-pyrrole ring), δ 7.49 (d, 4H, J = 7.60 Hz, Ar), 7.07 (dd, 1H), 6.98 (dd, 1H), 2.81 (s, 6H, CH_3), −4.20 (m, −NH). ^{11}B NMR (160 MHz, $CDCl_3$, δ in ppm): −0.66, ^{19}F NMR (470 MHz, $CDCl_3$, δ in ppm 25 °C): −149.33. ^{13}C NMR (100 MHz, $CDCl_3$, δ in ppm): 149.9, 139.6, 138.0, 135.9, 132.0, 131.5, 131.0, 130.7, 128.4, 125.1, 123.6, 121.7, 120.4, 120.1, 115.8, 114.2, 108.2, 21.7. HR-MS calcd for $C_{50}H_{38}BF_2N_7O$ *m/z* 801.3202, observed 801.3202.

4.7. Compound ***8***

A sample of BF_2-*meso*-pyrrolyl-25-oxasmaragdyrin **BF$_2$-3** (0.210 mmol) was dissolved in 40 mL $CHCl_3$ in a round bottom flask fitted with nitrogen gas inlet and outlet tubes. Pentafluorobenzaldehyde (0.108 mmol) was added to the reaction mixture and nitrogen gas was purged for 5 min. TFA (0.098 mmol) was added to initiate the reaction and stirring was continued for 24 h at room temperature. The reaction was quenched by addition of 0.1 M aqueous NaOH solution (20 mL) and extracted with dichloromethane. The organic layer was dried over Na_2SO_4 and concentrated under vacuum to afford crude product. The crude product was purified by column chromatography using petroleum ether/dichloromethane (60/40) and the pure compound was afforded as a greenish solid in 60% yield. ^{1}H NMR (700 MHz, $CDCl_3$, δ in ppm): 10.05 (d, 2H, J = 4.25 Hz, β-pyrrole H), 9.99 (d, 2H, J = 4.25 Hz, β-pyrrole H), 9.79 (d, 2H, J = 4.20 Hz, β-pyrrole H), 9.37 (s, 2H, β-furan H), 8.88 (d, 2H, J = 4.25 Hz, β-pyrrole H), 8.24 (d, 4H, J = 7.68 Hz, Ar), 7.68 (d, 1H, J = 3.24 Hz, *meso*-pyrrole ring), 7.61 (d, 4H, J = 7.70 Hz, Ar), 7.03 (dd, 1H, J = 3.24 Hz, *meso*-pyrrole ring), 6.90 (s, 1H, - CH), 2.17 (s, 6H, CH_3), −3.61 (m, −NH). ^{11}B NMR (128.37 MHz, $CDCl_3$, δ in ppm): −1.0, ^{19}F NMR (470 MHz, $CDCl_3$, δ in ppm, 25 °C): −141.40, −150.90, −155.85 and −161.28. ^{13}C NMR (100 MHz, $CDCl_3$, δ in ppm): 149.9, 137.9, 136.6, 135.1, 134.2, 132.2, 130.9, 130.6, 129.5, 128.8, 128.3, 128.1, 125.0, 123.8, 123.4, 121.9, 120.9, 120.3, 111.1, 107.1, 46.9, 29.5.

Conflicts of interest

There are no conflicts of interest to declare.

Acknowledgements

MR acknowledges the financial support provided by SERB (file no. EMR/2015/002196 to M.R.), Govt. of India and BU thanks UGC for fellowship.

Appendix A. Supplementary data

Supplementary data related to this article can be found at https://doi.org/10.1016/j.tet.2017.12.006.

References

1. Schmidt I, Jiao J, Thamyongkit P, Sharada DS, Bocian DF, Lindsey JS. *J Org Chem*. 2006;71:3033–3050.
2. Saltsman I, Goldberg I, Balasza Y, Gross Z. *Tetrahedron Lett*. 2007;48:239.
3. Xu L, Wen B, Kim G, et al. *Angew Chem Int Ed*. 2017;56:12322–12326.
4. Furuta H, Maeda H, Furuta T, Osuka A. *Org Lett*. 2000;2:187–189.
5. Maeda C, Shinokubo H, Osuka A. *Org Lett*. 2010;12:8.
6. (a) Santosh G, Ravikanth M. *Chem Phys Lett*. 2007;448:248;
   (b) Gross Z, Saltsmen I, Pandian RP, Barzilay C. *Tetrahedron Lett*. 1997;28:2383.
7. Santosh G, Ravikanth M. *Tetrahedron*. 2007;63:7833.
8. Gupta I, Ravikanth M. *J Chem Sci*. 2005;117:161.
9. Gupta I, Ravikanth M. *Tetrahedron Lett*. 2002;43:9453.
10. Rai S, Ravikanth M. *Tetrahedron*. 2007;63:2455.
11. Ghosh A, Butcher RJ, Mobin SM, Ravikanth M. *Acta Cryst*. 2010;66:1160–1161.
12. (a) Gupta I, Hung CH, Ravikanth M. *Eur J Org Chem*. 2003:4392;
   (b) Latos-Grazynski L, Lisowski J, Olmstead MM, Balch AL. *J Am Chem Soc*. 1987;109:4428.
13. Vollmer MS, Wurthner F, Effenberger F, et al. *Chem Eur J*. 1998;4:260.
14. Ono N, Miyagawa H, Ueta T, Ogawa T, Tani H. *J Chem Soc Perkin Trans*. 1998;1:1595.
15. Donatoni MC, Vieira YW, Brocksom TJ, Rabelo AC, Leite ER, de Oliveira KT. *Tetrahedron*. 2014;70:6963–6973.
16. Momo PB, Sampaio OM, Brocksom TJ, de Oliveira KT. *J Porphyrins Phthalocyanines*. 2015;19:745–752.
17. Momo PB, Pavani C, Baptista MS, Brocksom TJ, de Oliveira KT. *Eur J Org Chem*. 2014:4536–4547.
18. Arai Y, Segawa H. *Chem Commun*. 2010;46:4279–4281.
19. Bhyrappa P, Sankar M, Varghese B, Bhavana P. *J Chem Sci*. 2006;118:393–397.
20. Sun X, Zhang J, He B. *J. Photochem Photobiol A Chem*. 2005;172:283–288.
21. Kalita H, Kalita D, Lee WZ, Bellare J, Ravikanth M. *Chem Eur J*. 2014;33:10404.
22. Kalita H, Ravikanth M. *Chem Eur J*. 2015;21:7399.
23. Pareek Y, Ravikanth M, Chandrashekar TK. *Acc Chem Res*. 2012;45:1801.
24. Sridevi B, Narayanan SJ, Chandrashekar TK. *J Chem Sci*. 2000;112:422.
25. Bauer VJ, Clive DLJ, Dolphin D, et al. *J Am Chem Soc*. 1983;105:6429.
26. Sessler JL, Camiolo S, Gale PA. *Coord Chem Rev*. 2003;240:17.
27. Narayanan SJ, Sridevi B, Chandrashekar TK. *Org Lett*. 1999;4:587.
28. Rajeswara Rao M, Ravikanth M. *J Org Chem*. 2011;76:3582.
29. Kalita H, Lee WZ, Ravikanth M. *Inorg Chem*. 2014;53:9431.
30. Umasekhar B, Samantha P, Chatterjee T, Ravikanth M. *J Chem Sci*. 2016;128:1709.
31. Umasekhar B, Ganapathi E, Chatterjee T, Ravikanth M. *Dalton Trans*. 2015;44:16516.
32. Kim K, Jo C, Easwaramoorthi S, Sung J, Kim DH, Churchill DG. *Inorg Chem*. 2010;49:4881.
33. Khan TK, Jana SK, Rao MR, Shaikh MS, Ravikanth M. *Inorg Chim Acta*. 2012;383:257.
34. Heo PY, Lee CH. *Bull Kor Chem Soc*. 1996;17:515.